OXFORD

SOT | Society of Toxicology
www.toxsci.oxfordjournals.org

TOXICOLOGICAL SCIENCES, 154(2), 2016, 381–391

doi: 10.1093/toxsci/kfw175
Advance Access Publication Date: September 9, 2016
Research article

Coagulation-Driven Hepatic Fibrosis Requires Protease Activated Receptor-1 (PAR-1) in a Mouse Model of TCDD-Elicited Steatohepatitis

Rance Nault,[*,†] Kelly A. Fader,[*,†] Anna K. Kopec,[†,‡] Jack R. Harkema,[‡] Timothy R. Zacharewski,[*,†] and James P. Luyendyk[†,‡,1]

[*]Department of Biochemistry & Molecular Biology, Michigan State University, East Lansing, Michigan; [†]Institute for Integrative Toxicology, Michigan State University, East Lansing, Michigan; and [‡]Department of Pathobiology & Diagnostic Investigation, Michigan State University, East Lansing, Michigan

[1]To whom correspondence should be addressed. 1129 Farm Lane, Rm. 253, East Lansing, Michigan 48824-1319. E-mail: luyendyk@cvm.msu.edu.

ABSTRACT

Emerging evidence supports a role for environmental chemical exposure in the pathology of non-alcoholic fatty liver disease (NAFLD), a disease process tightly linked to increased activity of the blood coagulation cascade. Exposure of C57BL/6 mice to the persistent environmental contaminant 2,3,7,8-tetrachlorodibenzo-*p*-dioxin (TCDD) recapitulates features of the NAFLD spectrum, including steatosis, hepatic injury, inflammation, and fibrosis. We assessed coagulation cascade activation, and determined the role of the thrombin receptor protease activated receptor-1 (PAR-1) in experimental TCDD-elicited NAFLD. Chronic exposure to TCDD (30 μg/kg every 4 days for 28 days) was associated with intrahepatic coagulation, indicated by increased plasma thrombin-antithrombin levels and hepatic fibrin(ogen) deposition. PAR-1 deficiency diminished TCDD-elicited body weight loss and relative liver weight was reduced in TCDD-exposed PAR-1$^{-/-}$ mice compared with TCDD-exposed wild-type mice. PAR-1 deficiency did not affect TCDD-induced hepatic steatosis or hepatocellular injury, as indicated by serum alanine aminotransferase activity. Despite a lack of effect on these 2 features of NAFLD pathology, PAR-1 deficiency was associated with a reduction in hepatic inflammation evident in liver histopathology, and reflected by a reduction in serum levels of the proinflammatory cytokine interleukin-6. Moreover, TCDD-driven hepatic collagen deposition was markedly reduced in PAR-1-deficient mice. These results indicate that experimental TCDD-elicited steatohepatitis is associated with coagulation cascade activation and PAR-1-driven hepatic inflammation and fibrosis.

Key words: TCDD; Coagulation; PAR-1; Fibrosis; NAFLD.

The worldwide incidence of non-alcoholic fatty liver disease (NAFLD) is continuously increasing, affecting over 35% of the US population alone (Ford *et al.*, 2010; Vanni *et al.*, 2010). Several factors, including genetics, diet, lifestyle, and age, have been implicated in the development of NAFLD and associated metabolic disorders including diabetes, dyslipidemia, and cardiovascular disease (Pitsavos *et al.*, 2006; Unger and Scherer, 2010; Unger *et al.*, 2010). Recent studies also suggest exposure to environmental contaminants including persistent organic pollutants and organochlorines contributes to metabolic disease development (Cave *et al.*, 2010; Lee *et al.*, 2006, 2007; Taylor *et al.*, 2013). For example, 2,3,7,8-tetrachlorodibenzo-*p*-dioxin (TCDD), the prototypical aryl hydrocarbon receptor (AhR) ligand, has been shown to contribute to the progression of NAFLD spectrum from simple, reversible steatosis, to steatohepatitis and early signs of fibrosis in mice (Kopec *et al.*, 2013; Nault *et al.*, 2015a; Pierre *et al.*, 2014). Notably, all of these pathologies are elements of the NAFLD spectrum in humans. Activation of the AhR, a

basic helix–loop–helix transcription factor, results in the dissociation of chaperone proteins, nuclear translocation, and dimerization with the AhR nuclear translocator (ARNT). The TCDD–AhR–ARNT complex then binds to dioxin response elements, and elicits changes in gene expression. Studies in AhR null mice strongly indicate that the impact of TCDD on NAFLD features, such as hepatic lipid accumulation, is driven by AhR activation (Fernandez-Salguero *et al.*, 1996).

Development of liver diseases such as the NAFLD has been associated with tissue factor (TF)-dependent activation of the blood coagulation cascade (Kassel *et al.*, 2011; Owens *et al.*, 2012). Coagulation cascade activation results in generation of the serine protease thrombin, which cleaves soluble fibrinogen leading to deposition of insoluble fibrin polymers in the liver (Kassel *et al.*, 2011). Thrombin also triggers intracellular signaling in numerous hepatic nonparenchymal cells (eg, macrophages, stellate cells) through activation of the protease activated receptor-1 (PAR-1; *F2r*). Thrombin activation of PAR-1 has been shown to drive multiple NAFLD-associated pathologies, including hepatic lipid accumulation, inflammation and hepatocellular injury, depending on the experimental setting (Kassel *et al.*, 2011, 2012; Kopec *et al.*, 2014; Luyendyk *et al.*, 2010). Notably, PAR-1 activation promotes stellate cell activation *in vitro* (Fiorucci *et al.*, 2004; Gaca *et al.*, 2002), and hepatic fibrosis is reduced in PAR-1$^{-/-}$ mice challenged chronically with hepatocellular or biliary toxicants (Sullivan *et al.*, 2010). Collectively, these studies indicate a central role for coagulation and thrombin signaling across the spectrum of NAFLD/NASH pathologies.

Repeated TCDD exposure in mice has been shown to promote the development of steatosis, steatohepatitis, and fibrosis (Fader *et al.*, 2015; Nault *et al.*, 2015a; Pierre *et al.*, 2014). However, no studies have examined whether the progression of liver pathologies elicited by TCDD is coupled to coagulation cascade activation, and the role of PAR-1 in this experimental context is unknown. Consequently, we determined whether coagulation cascade activation accompanies TCDD-elicited hepatotoxicity and utilizing PAR-1$^{-/-}$ mice tested the hypothesis that progression of NAFLD-associated pathologies involves the thrombin receptor PAR-1.

MATERIALS AND METHODS

Animals

Age-matched male PAR-1$^{-/-}$ (Connolly *et al.*, 1997) and PAR-1$^{+/+}$ mice, both on an N8 C57BL/6J background, were obtained by homozygous breeding as previously described (Luyendyk *et al.*, 2011). Mice used in the study were between 12 and 16 weeks of age and studies were performed in duplicate. All mice were housed in Innovive cages (Innovive Inc., San Diego, California) with alpha-dri bedding (Shepherd Specialty Papers, Milford, New Jersey) at 30-40% humidity and a 12 h light/dark cycle. Animals were fed *ad libitum* (Harlan Teklad 22/5 Rodent Diet 8940, Madison, Wisconsin) and had free access to Aquavive acidified water (Innovive Inc.). In both studies, mice were gavaged every 4 days (d) for 28 d (a total of 7 exposures) with sesame oil vehicle (Sigma-Aldrich, St. Louis, Missouri) or 30 μg/kg TCDD (AccuStandard, New Haven, Connecticut; 99.8% purity) in sesame oil with a volume of 100 μL. Doses were chosen based on previous studies suggesting that these potentially reflect the lifetime exposure to TCDD and related compounds in humans (Nault et al., 2016). 28 d following the initial dose, animals were anesthetized using isoflurane, plasma, and serum were collected from the caudal *vena cava* using a syringe with and without sodium citrate (0.38% final), respectively, and stored at –80 °C. Livers were collected, weighed, and frozen in liquid nitrogen and stored at –80 °C or fixed in 10% neutral buffered formalin (Sigma-Aldrich) for histological processing. All procedures were approved by the Michigan State University All-University Committee on Animal Use and Care.

Serum clinical chemistry

Serum alanine aminotransferase (ALT) activity was determined using a commercially available reagent (Infinity ALT/GPT; Thermo Fisher, Waltham, Massachusetts). Thrombin–antithrombin (TAT) levels in the plasma were determined using a commercial enzyme-linked immunosorbent assay kit (Enzygnost TAT micro; Siemens Healthcare Diagnostics, Deerfield, Illinois). Assays were performed using an infinite M200 plate reader (Tecan, Durham, North Carolina). Serum cytokine levels were determined using the Meso Scale V-PLEX Proinflammatory panel kit and Sector S 600 (Meso Scale Discovery, Rockville, Maryland).

Histopathology

All histological processing and staining were performed at the Michigan State University Investigative Histopathology Laboratory (https://humanpathology.natsci.msu.edu/; last accessed September 14, 2016) (Nault *et al.*, 2015a). Briefly, frozen livers were sectioned at 6 μm and stained with an Oil Red O (ORO) solution and Gill 2 hematoxylin counterstain. Formalin-fixed paraffin-embedded sections were stained for collagen using PicroSirius Red (PSR), hematoxylin & eosin (H&E), and immunohistochemically for fibrin(ogen) as described previously (Joshi *et al.*, 2016). In brief, fibrin(ogen) was stained using a polyclonal rabbit anti-human fibrin(ogen) antibody (Dako, Carpinteria, California) at a dilution of 1:200, and detected using biotinylated goat anti-rabbit IgG with Vectastain R.T.U. Elite ABC reagent and Vector Nova Red Peroxidase substrate (Vector Laboratories, Burlingame, California). Tissues were then counterstained with Gill 2 hematoxylin. Slides were digitized using an Olympus Virtual Slide System (VS110) at 20x magnification and images were sampled using the Visiomorph Microimager (Visiopharm, Denmark). Quantitation of histological features was performed using an in-house developed tool (Nault *et al.*, 2015a). Semi-quantitative severity scoring of H&E-stained liver sections was performed by a board certified veterinary pathologist experienced in hepatic toxicologic pathology of laboratory rodents. The pathologist examined the slides without previous knowledge of the individual exposure history of the mice. Criteria used for scoring the severity of the individual microscopic lesions (ie, hepatocellular vacuolization, cellular inflammation, and bile duct hyperplasia) were (1) less than 10% of tissue affected (minimal), (2) 10–33% of tissue affected (mild), (3) 33–66% of tissue affected, and (4) greater than 66% of tissue affected (marked).

RNA extraction and gene expression analysis

Total RNA was extracted from 100 mg liver sections in 1.3 mL TRIzol (Life Technologies, Carlsbad, California), with an additional phenol:chloroform extraction, as previously described (Nault *et al.*, 2015b). RNA was stored in RNA storage solution (Life Technologies) and assessed for purity by Nanodrop (A_{260}/A_{280} ratio; Thermo Scientific). Synthesis of cDNA was performed using 1 μg of RNA, High Capacity cDNA Reverse Transcription kit (Applied Biosystems), and MyCycler thermal cycler (Bio-Rad).

Quantitative real-time PCR (qPCR) was performed using SYBR Green master mix (Bio-Rad) and a CFX96 Real-Time PCR Detection System (Bio-Rad). The expression of each gene was normalized to the geometric mean of *Actb*, *Gapdh*, and *Hprt* and differential expression was calculated using the $2^{-\Delta\Delta CT}$ method. Primer sequences are provided in Supplementary Table S1.

Statistics

Statistical analyses were performed using R version 3.2.2 (R Foundation for Statistical Computing) and consisted of Student's *t*-test for comparison of 2 groups. A 2-way ANOVA with treatment and genotype as factors was used for evaluation of genotype and treatment effects followed by Student–Newman–Keul's *post-hoc* test. Differences were considered significant when $P \leq .05$. Data from 2 independent studies were combined for body and liver weights, as well as ALT measurements. All other figures represent values for one independent study.

RESULTS

TCDD Exposure Activates the Coagulation Cascade

Activation of the coagulation cascade is coupled to the development and progression of NAFLD pathologies (Kassel *et al.*, 2011; Owens *et al.*, 2012). Notably, repeated exposure to TCDD in wild-type mice significantly increased plasma thrombin–antithrombin (TAT) levels, a stable biomarker of coagulation cascade activation (Fig. 1A). Consistent with increased thrombin proteolytic activity (Fig. 1B), TCDD-exposed mice had a significant increase in the amount of intrahepatic fibrin(ogen), largely located in the hepatic portal areas (Fig. 1C). These results indicate that repeated exposure to TCDD increases intrahepatic coagulation in mice.

PAR-1 Deficiency Does Not Reduce TCDD-Elicited Hepatotoxicity

Coagulation-driven steatohepatitis is mediated in part through activation of PAR-1 (Kassel *et al.*, 2011; Owens *et al.*, 2012). We have previously observed that PAR-1 expression is induced in livers of mice exposed repeatedly to TCDD (Nault *et al.*, 2015b). To determine the role of PAR-1 in TCDD-elicited liver pathology, we utilized PAR-$1^{-/-}$ mice. Overall, unexpected mortalities were observed only in the wild-type TCDD treated animals (5/16), whereas no mortality occurred in PAR-$1^{-/-}$ mice. Noting protection from overt TCDD toxicity, TCDD-mediated weight loss was significantly reduced in PAR-$1^{-/-}$ mice compared with wild-type mice (Fig. 2A). The weight loss was observed beginning at ~15 days (4 exposures) in 2 independent experiments (Supplementary Fig. S1). Concomitantly, an increase in relative

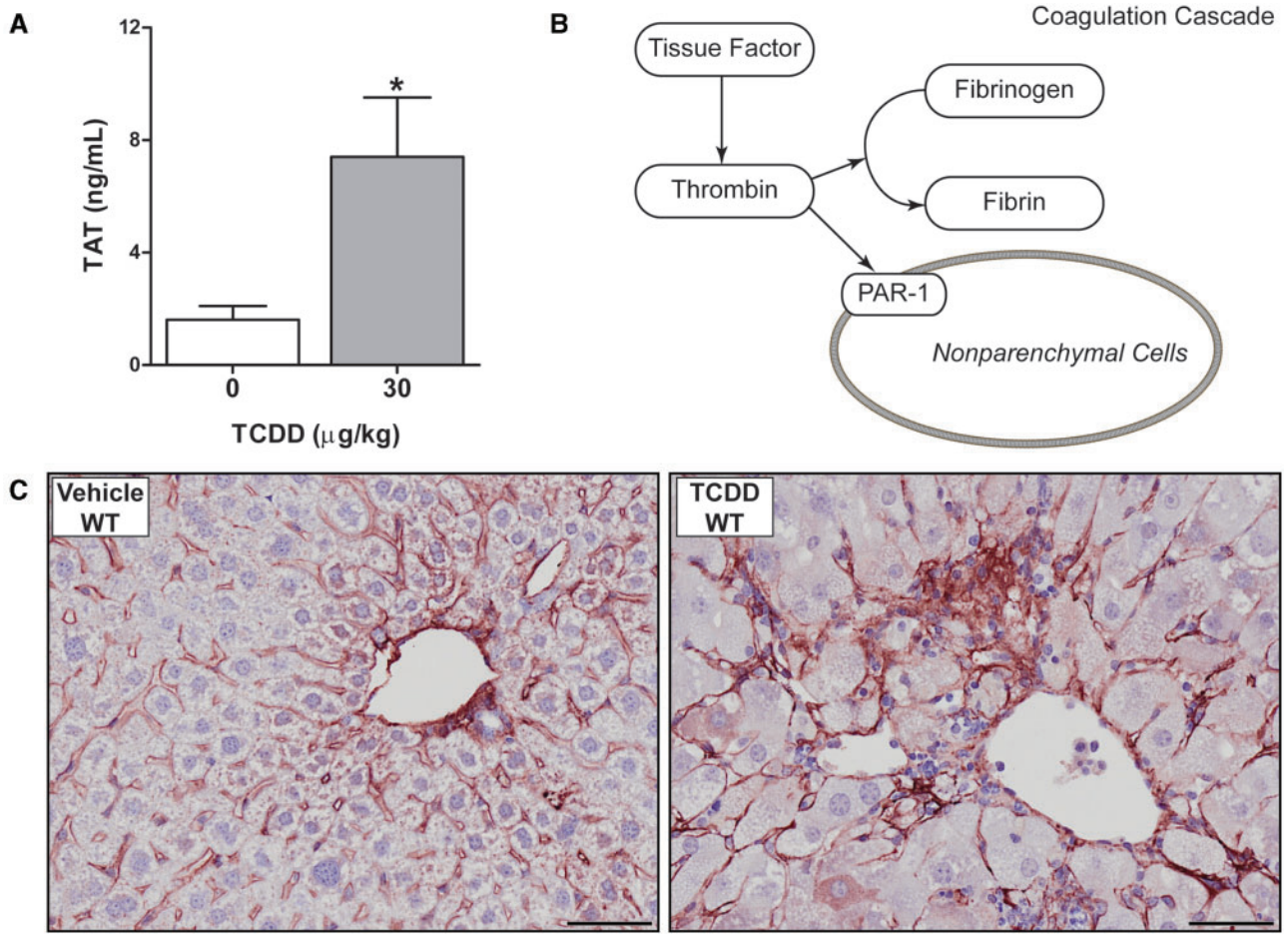

FIG. 1. Activation of the coagulation cascade in livers of male wild-type mice gavaged with sesame oil vehicle or 30 μg/kg TCDD every 4 days for 28 days. (A) Plasma thrombin antithrombin (TAT) levels are represented as mean + SEM for $N = 6$ (vehicle) or $N = 8$ (TCDD). (B) Overview of the coagulation cascade describes the relationship between fibrin deposition and activation of the protease activated receptor-1 (PAR-1) describing the pathway being investigated in response to TCDD exposure. (C) Representative photomicrographs of liver sections stained for fibrin(ogen) (red) in vehicle and TCDD-treated mice. Asterisks indicate a significant difference ($P \leq 0.05$) determined by Student's *t*-test and scale bars represent 50 μm.

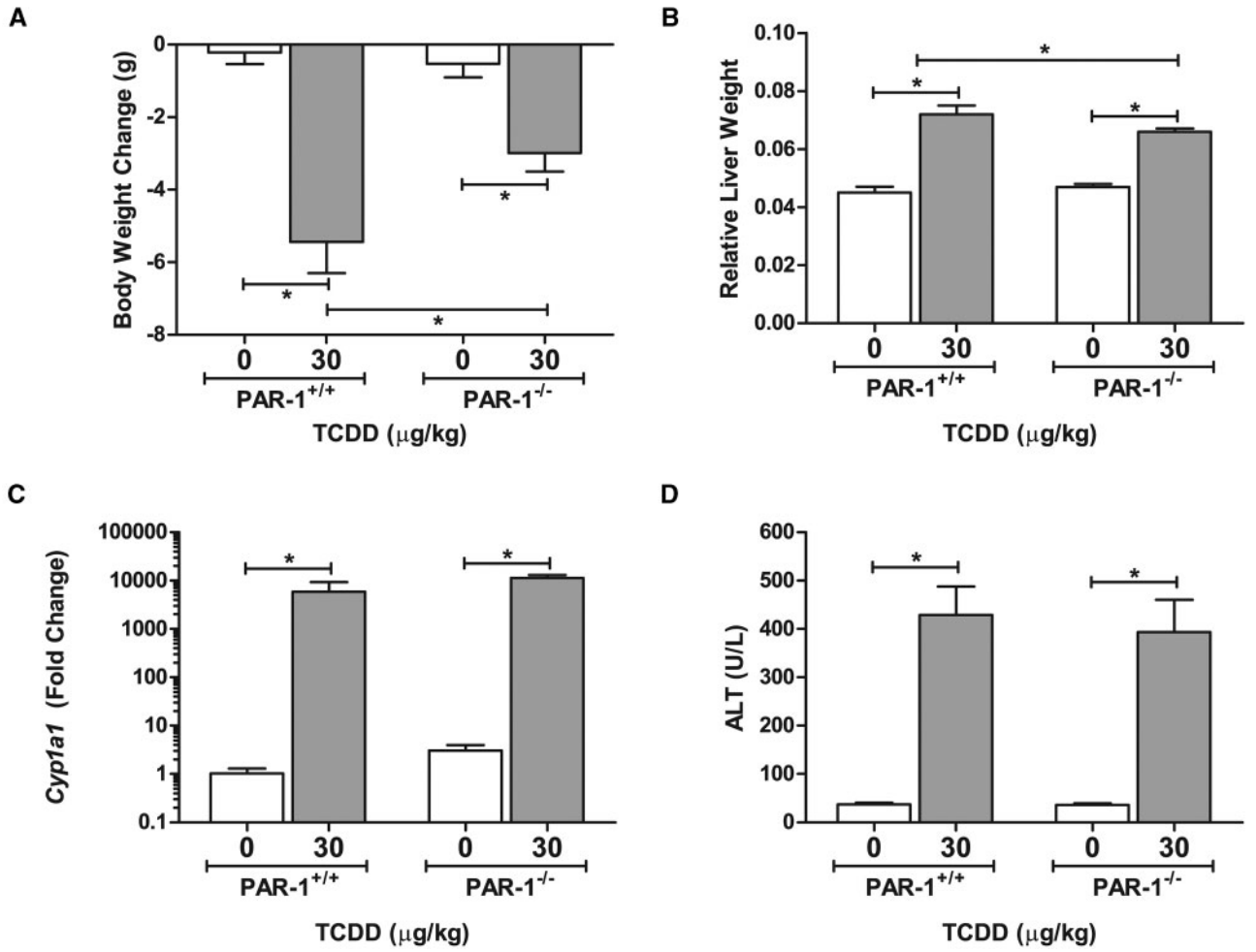

FIG. 2. Effect of PAR-1 deficiency on markers of TCDD-induced toxicity. TCDD-elicited changes in (A) body weight (B) relative liver weight (liver weight/body weight), (C) hepatic *Cyp1a1* expression, and (D) serum ALT levels were determined in male wild-type (PAR-$1^{+/+}$) and PAR-$1^{-/-}$ mice gavaged with sesame oil vehicle or 30 μg/kg TCDD every 4 days for 28 days. Bars represent mean + SEM. Lines with an asterisk (*) above indicate a significant difference ($P \leq 0.05$) within and/or between genotype determined by a 2-way ANOVA followed by Student–Newman–Keul's *post hoc* test. Sample sizes (N) are 9 (PAR-$1^{+/+}$ vehicle), 8 (PAR-$1^{+/+}$ TCDD), 7 (PAR-$1^{-/-}$ vehicle), and 11 (PAR-$1^{-/-}$ TCDD). For qPCR of *Cyp1a1* sample sizes (N) are 4 (PAR-$1^{+/+}$ vehicle), 5 (PAR-$1^{+/+}$ TCDD), 3 (PAR-$1^{-/-}$ vehicle), and 6 (PAR-$1^{-/-}$ TCDD).

liver weight (liver weight/body weight ratio) was observed in TCDD-treated animals although to a lesser extent in PAR-$1^{-/-}$ mice increasing 1.6- and 1.4-fold in PAR-$1^{+/+}$ and PAR-$1^{-/-}$ mice, respectively (Fig. 2B). Absolute liver weights increased similarly (Supplementary Fig. S2). Induction of hepatic *Cyp1a1* expression was similar in wild-type and PAR-$1^{-/-}$ mice suggesting equivalent AhR activation in both genotypes (Fig. 2C). Of importance, serum ALT activity, a marker of hepatocellular injury, increased in TCDD-exposed wild-type mice (Fig. 2D). This increase was similar in TCDD-exposed PAR-$1^{-/-}$ mice (Fig. 2D), indicating equivalent hepatotoxicity in both genotypes as a result of repeated TCDD exposure. Increases in ALT were observed in the absence of evidence of hepatocyte necrosis by histological evaluation.

Impact of PAR-1 Deficiency on the Development of NAFLD

Evaluation of hepatic lipid accumulation was performed by quantification of Oil Red O-stained liver sections (Fig. 3A), an approach shown previously to correlate with hepatic triglyceride levels (Levene *et al.*, 2012). Wild-type and PAR-$1^{-/-}$ mice developed panacinar micro- and macrovesicular steatosis of similar severity (Fig. 3A and B). Examination of H&E-stained liver sections identified TCDD-induced periportal inflammation characterized by a mixed inflammatory cell response composed of neutrophilic granulocytes and mononuclear leukocytes (lymphocytes and monocytes) and occasional eosinophils in both wild-type and PAR-$1^{-/-}$ mice exposed to TCDD. Markedly less periportal inflammation and bile duct proliferation was observed in PAR-$1^{-/-}$ mice (Fig. 4 and Table 1). Interestingly, the increase in plasma TAT level was also attenuated in TCDD-exposed PAR-$1^{-/-}$ mice (3.4 ± 0.5 ng/ml [TCDD] vs 1.4 ± 0.3 ng/ml [vehicle]) compared with PAR-$1^{+/+}$ mice (7.4 ± 2.1 ng/ml [TCDD] vs 1.6 ± 0.5 ng/ml [vehicle]), consistent with known crosstalk between coagulation and inflammation pathways (Esmon, 2005). Plasma levels of IFN-γ, IL-10, IL-6, and TNFα increased in both wild-type and PAR-$1^{-/-}$ mice exposed to TCDD (Fig. 5). Notably, IFN-γ and IL-6 in TCDD-treated PAR-$1^{-/-}$ mice were increased and reduced, respectively, compared with their wild-type counterparts (Fig. 5A and C). Specifically, IFN-γ increased to 1.75 ± 0.06 and 3.81 ± 0.40 pg/mL whereas IL-6 increased to 71.21 ± 11.30 and only 32.53 ± 5.01 pg/mL in wild-type and PAR-$1^{-/-}$ mice, respectively, revealing dichotomous effects on these cytokines.

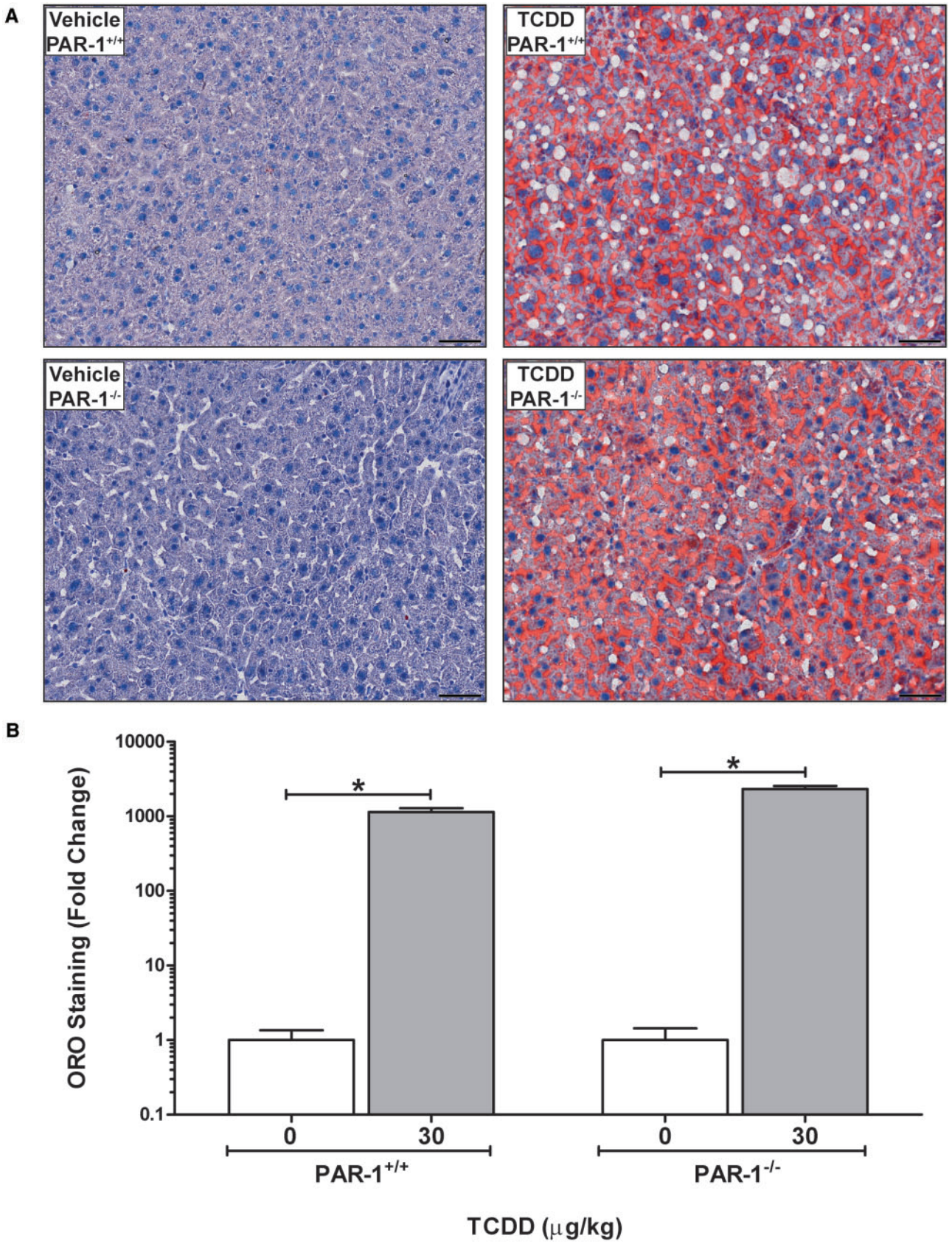

FIG. 3. Hepatic lipid accumulation in male mice gavaged with sesame oil vehicle or 30 μg/kg TCDD every 4 days for 28 days. (A) Representative photomicrographs of liver sections stained with Oil Red O (ORO). Scale bars represent 50 μm. (B) Quantitation of ORO staining is represented as mean + SEM for N = 4 (PAR-$1^{+/+}$ vehicle), 5 (PAR-$1^{+/+}$ TCDD), 3 (PAR-$1^{-/-}$ vehicle) and 6 (PAR-$1^{-/-}$ TCDD). Lines with an asterisks (*) above indicate a significant difference ($P \leq 0.05$) within genotypes determined by 2-way ANOVA followed by Student–Newman–Keul's *post hoc* test. No difference was observed between genotypes.

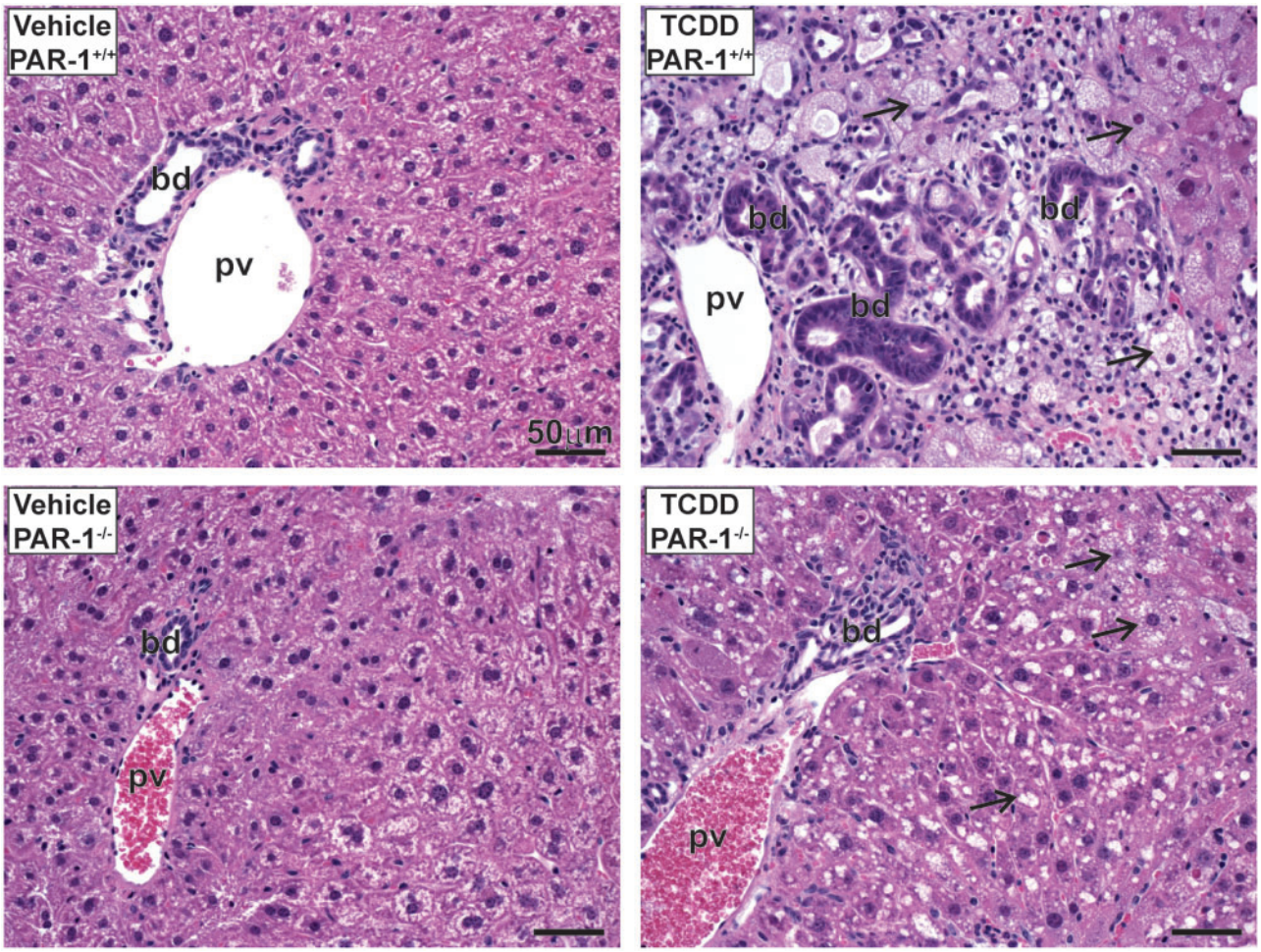

FIG. 4. Light photomicrographs of hematoxylin and eosin (H&E)-stained liver tissue sections from male mice gavaged with sesame oil vehicle or 30 μg/kg TCDD every 4 days for 28 days. Marked bile duct (bd) hyperplasia, hepatocellular vacuolization (arrows), and periportal inflammatory cell infiltration in the liver is shown. Pv indicates the portal vein. Scale bars represent 50 μm.

TABLE 1. Semi-Quantitative Scoring of H&E Stained Liver Sections.

TCDD (μg/kg)	Genotype	Vacuolization[a]	Inflammation[a]	Bile Duct Proliferation[a]
0	PAR-1$^{+/+}$	0.0 ± 0.0	0.0 ± 0.0	0.0 ± 0.0
30		4.0 ± 0.0	3.6 ± 0.2	2.6 ± 0.6
0	PAR-1$^{-/-}$	0.0 ± 0.0	0.0 ± 0.0	0.0 ± 0.0
30		3.0 ± 0.3	2.2 ± 0.2	0.4 ± 0.4

[a]H&E stained liver sections were semi-quantitatively scored from 0 to 4; 0—no findings, 1—minimal, 2—mild, 3—moderate, 4—marked. A total of 5 slides were evaluated for each group with the exception of vehicle PAR-1$^{-/-}$ mice in which 4 slides were evaluated. Scoring criteria are described in the materials and methods. Values represent mean +/− SEM.

Development of periportal fibrosis as indicated by excess collagen deposition was determined by qualitative and quantitative assessment of PSR-stained liver sections. In agreement with previous studies (Nault *et al.*, 2015a; Pierre *et al.*, 2014), TCDD treatment significantly increased collagen deposition in the liver (Fig. 6A and B). The TCDD-induced fibrosis in wild-type mice that was associated with the periportal inflammation and bile duct hyperplasia, often extended from the periportal regions to the liver capsule. Notably, collagen deposition was significantly reduced in PAR-1$^{-/-}$ mice, and was largely confined to portal regions (Fig. 6A and B). Concomitant with the reduction in collagen deposition there was a dramatic reduction in the TCDD-driven bile duct proliferation in PAR-1$^{-/-}$ mice (Table 1).

DISCUSSION

Activation of the coagulation cascade is tightly linked to the development of NAFLD-associated pathologies, particularly steatohepatitis and fibrosis (Kassel *et al.*, 2011; Owens *et al.*, 2012). Here, we found that subchronic TCDD exposure is also coupled to increased intrahepatic coagulation, marked by increased thrombin generation and hepatic fibrin(ogen) deposition. Notably, the pattern of fibrin(ogen) deposition in TCDD-exposed mice was distinct from that observed in other models of liver toxicity and disease, wherein the pattern of deposition is often coupled to the site of injury (Kopec and Luyendyk, 2016). A role for fibrin(ogen) deposits in TCDD-elicited pathology cannot be ruled out, as additional studies are required to define the role of fibrin(ogen) deposits in this experimental context. Our prior identification of increased PAR-1 mRNA expression in TCDD-exposed mice suggested a potential role for thrombin signaling in TCDD-elicited pathology. Indeed, here we report for

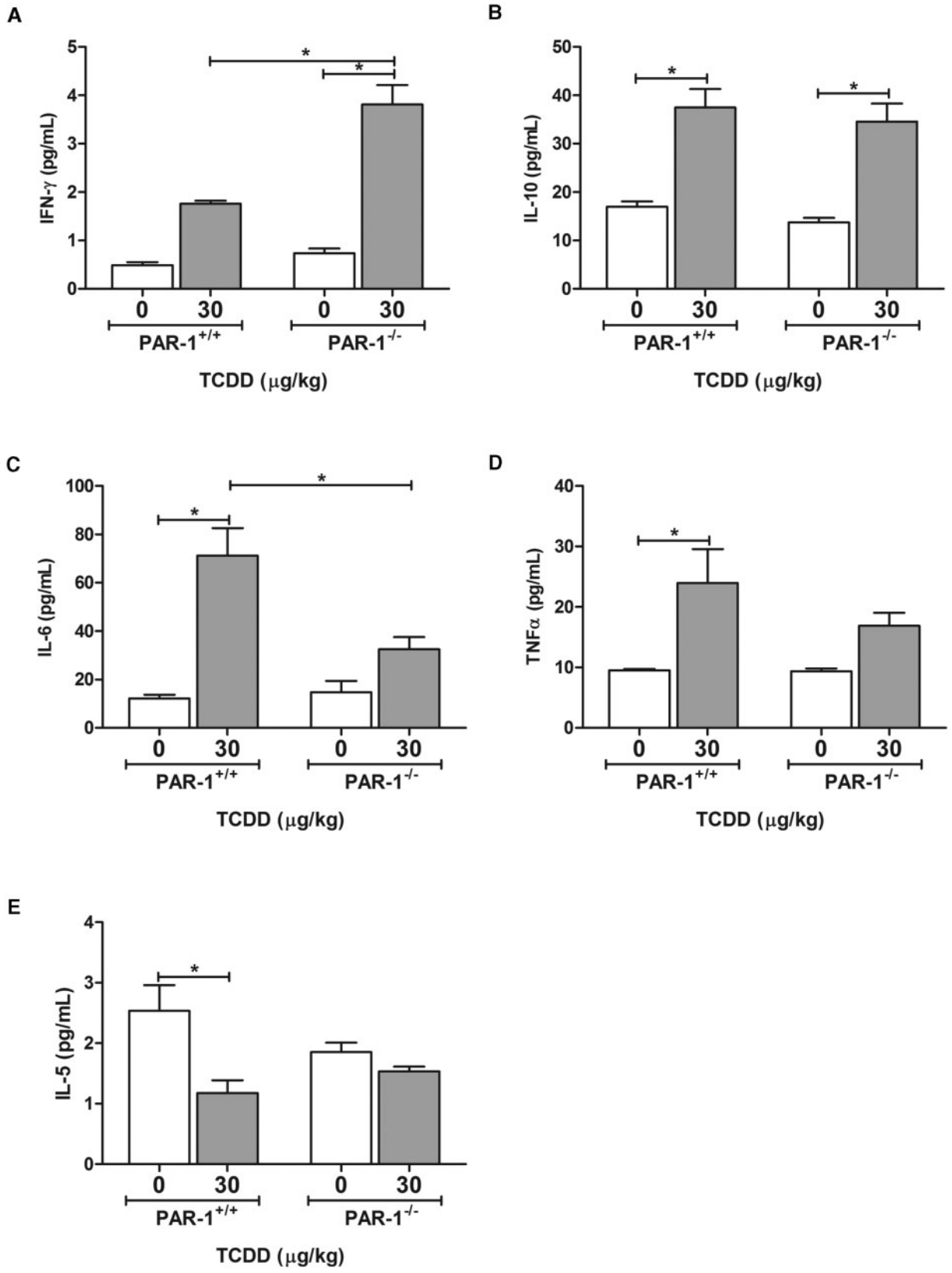

FIG. 5. TCDD-elicited changes in serum (A) IFN-γ, (B) IL-10, (C) IL-6, (D) TNFα, and (E) IL-5 levels in male wild-type (PAR-$1^{+/+}$) and PAR-$1^{-/-}$ mice gavaged with sesame oil vehicle or 30 μg/kg TCDD every 4 days for 28 days. Bars represent mean + SEM for N = 4 (PAR-$1^{+/+}$ vehicle), 5 (PAR-$1^{+/+}$ TCDD), 3 (PAR-$1^{-/-}$ vehicle) and 6 (PAR-$1^{-/-}$ TCDD). Lines with an asterisk (*) indicate a significant difference ($P \leq 0.05$) within and/or between genotype determined by 2-way ANOVA followed by Student–Newman–Keul's *post hoc* test.

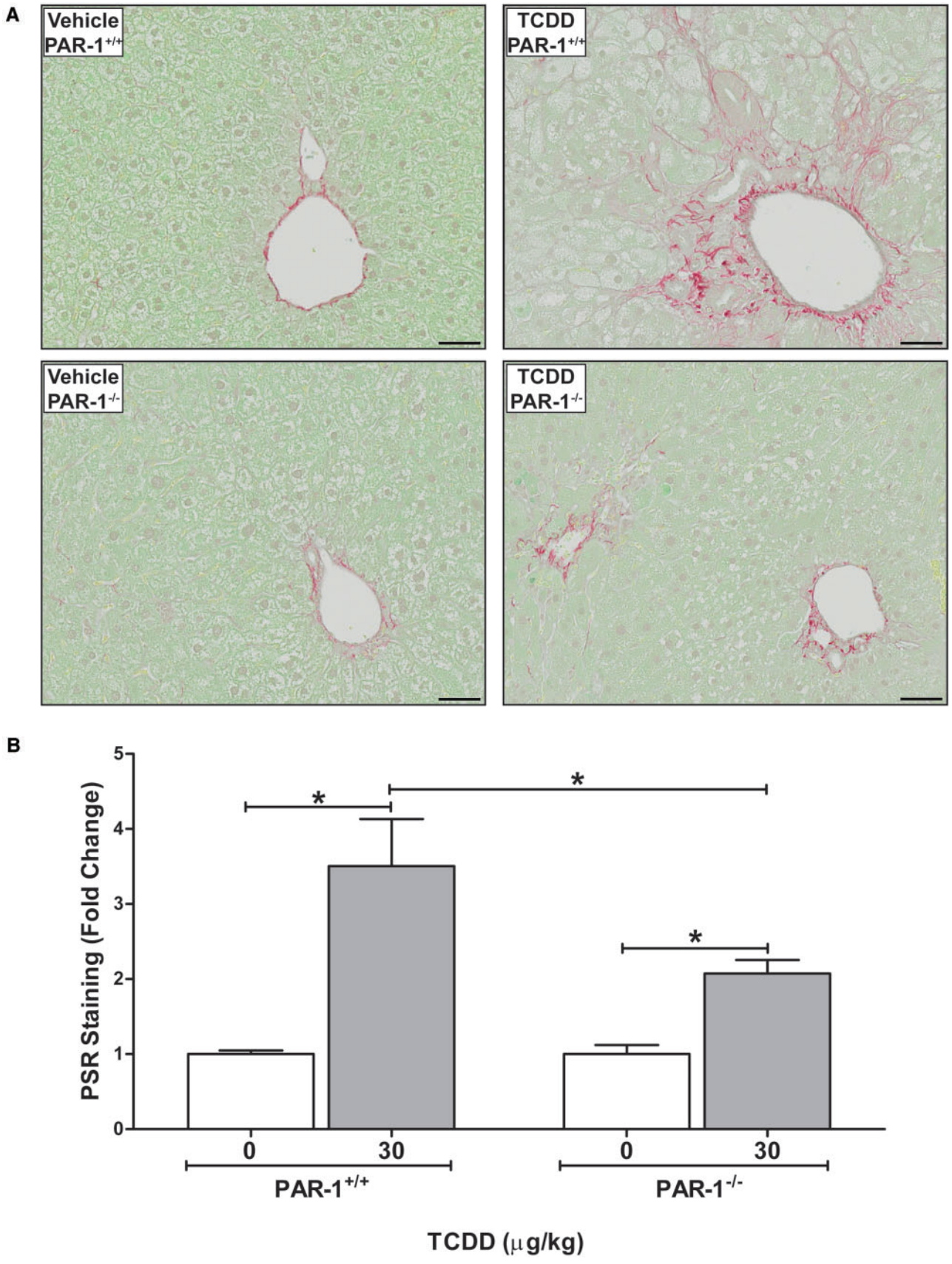

FIG. 6. Hepatic collagen deposition in male mice gavaged with sesame oil vehicle or 30 μg/kg TCDD every 4 days for 28 days. (A) Representative photomicrographs of liver sections stained with PicroSirius Red (PSR) in wild-type and PAR-1$^{-/-}$ vehicle and TCDD-treated mice. Scale bars represent 50 μm. (B) Quantitation of PSR staining is represented as mean + SEM for N = 5 (PAR-1$^{+/+}$ vehicle), 3 (PAR-1$^{+/+}$ TCDD), 4 (PAR-1$^{-/-}$ vehicle) and 4 (PAR-1$^{-/-}$ TCDD). Lines with an asterisks (*) above indicates a significant difference ($P \leq 0.05$) within and/or between genotype determined by 2-way ANOVA followed by Student–Newman–Keul's *post hoc* test.

the first time that PAR-1 activation plays a central role in hepatic fibrosis driven by chronic TCDD exposure.

TCDD is a well-known hepatotoxicant and chronic exposure has been reported to result in weight loss (wasting) and increased relative liver weight. Notably, both of these changes were diminished in TCDD-exposed PAR-$1^{-/-}$ mice, indicating that PAR-1 plays an important role in TCDD toxicity. To the best of our knowledge, this is the first report of thrombin signaling driving systemic toxicity of an environmentally relevant xenobiotic. PAR-1 is expressed by numerous cells in multiple tissues and the precise cellular source of PAR-1 in control of TCDD-mediated weight loss is a question for future study. Although PAR-1 plays a central role in the activation of human platelets, it is not expressed by mouse platelets (Kahn *et al.*, 1999). Thus, whereas TCDD has been shown to impact platelet activation (Lindsey *et al.*, 2014), our observations in PAR-$1^{-/-}$ mice cannot be ascribed to thrombin-mediated platelet activation. Notably, hepatic induction of classic AhR target genes (eg, *Cyp1a1*) in TCDD-exposed mice was not affected by PAR-1 deficiency, implying that protection from disease is not likely due to failed AhR activation.

Analogous to PAR-$1^{-/-}$ mice on a methionine-choline-deficient (MCD) diet-fed mice, PAR-1 deficiency had no effect on the development of hepatic steatosis in TCDD-exposed mice. Notably, this contrasts findings in models of NAFLD driven by diets high in fat, where PAR-1 deficiency largely prevents hepatic steatosis in the absence of effects on body weight (Kassel *et al.*, 2011). Although the basis for this difference is not clear, it is possible that TCDD (and MCD challenge alike) alter normal metabolic function in liver leading to excess hepatic lipid accumulation irrespective of caloric intake. In contrast to MCD diet-challenged mice, PAR-1 deficiency had no effect on hepatocellular injury caused by TCDD as indicated by similarly increased serum ALT levels in TCDD-treated wild-type and PAR-$1^{-/-}$ mice. Thus, whereas PAR-1 driven hepatocellular injury is disconnected from hepatic steatosis in MCD diet-challenged mice, it appears that lipid accumulation and hepatocellular injury are PAR-1-independent in TCDD-exposed mice.

In agreement with the role of PAR-1 in promoting hepatic inflammation in experimental MCD diet-driven steatohepatitis, serum levels of the proinflammatory cytokine IL-6 were reduced in TCDD-exposed PAR-$1^{-/-}$ mice. Similarly, TCDD exposure increased serum TNFα levels in wild-type mice, but did not increase these levels in PAR-$1^{-/-}$ mice. This was coupled with a reduction in hepatic inflammation as assessed by histopathology. Interestingly, this is a potential mechanistic disconnect between hepatic injury and the inflammatory response in TCDD-exposed mice, as serum ALT levels were not reduced in PAR-$1^{-/-}$ mice. Characterization of the precise changes in hepatic cytokine expression and inflammatory cell accumulation driven by PAR-1 in TCDD-exposed, particularly in the context of cell-specific changes in oxidative stress, should form the next step of investigation in this experimental setting. However, it is intriguing to note that cytokine levels were not unilaterally reduced in PAR-$1^{-/-}$ mice. For example, serum IFN-γ expression increased in TCDD-exposed PAR-$1^{-/-}$ mice compared with wild-type mice. Although its role is certainly context-dependent, in some experimental settings IFN-γ is noted to have antifibrotic activity through induction of stellate cell quiescence and apoptosis (Weng *et al.*, 2007). Additional studies are required to define the cellular source of IFN-γ and its role in the TCDD-induced steatohepatitis.

Interestingly, our studies show a robust increase in hepatic fibrosis in mice exposed chronically to TCDD, and identify PAR-1 signaling as an important contributor to hepatic fibrosis in this setting. Of importance, the reduction in hepatic fibrosis in PAR-$1^{-/-}$ mice could not be attributed to a reduction in hepatic steatosis or hepatocellular injury. This is analogous to fibrosis driven by chronic exposure to another hepatotoxic xenobiotic, carbon tetrachloride (CCl_4). In that model, thrombin signaling does not impact CCl_4 hepatotoxicity, but nevertheless contributes to the progression of fibrosis (Rullier *et al.*, 2008). Cell culture studies indicate thrombin has direct profibrogenic effects on stellate cells *in vitro*, suggesting that local thrombin generation driven by TCDD hepatotoxicity could directly promote fibrogenesis by activation of PAR-1 on stellate cells. However, to date, there are no studies definitively identifying a profibrogenic role for PAR-1 expressed by stellate cells *in vivo*. Indeed, an equally intriguing possibility is that PAR-1 drives hepatic inflammation via macrophage activation, and that this indirectly promotes stellate cell activation. Indeed, bone-marrow transplant studies suggest a role for hematopoietic cell PAR-1 in CCl_4-induced hepatic fibrosis (Kallis *et al.*, 2014). Alternatively, the reduction in fibrosis may be coupled to the observed reduction in bile duct proliferation in PAR-1-deficient mice. TCDD exposure was previously reported to cause bile duct proliferation (Vos *et al.*, 1974), although the mechanism remains elusive. Our results suggest that TCDD-mediated bile duct proliferation may be driven indirectly by thrombin activation of PAR-1. Indeed, previous studies demonstrated that PAR-1 signaling on bile duct epithelial cells contributes to experimental xenobiotic-induced bile duct fibrosis by enhancing $\alpha_V\beta_6$-mediated TGFβ activation (Sullivan *et al.*, 2010, 2011).

In summary, we demonstrate that following chronic TCDD exposure, activation of the coagulation cascade drives hepatic inflammation and fibrosis, independent of hepatic lipid accumulation and injury, through a PAR-1-dependent mechanism. These studies are an important example of changes reactive to tissue injury, such as coagulation, driving penultimate pathologies associated with chronic chemical exposure. The observation that PAR-1 deficiency decreases inflammation and fibrosis without affecting steatosis is significant, insofar as it suggests a mechanism of disease progression apparently independent of underlying lipid metabolism. Comparison of these results to the role of PAR-1 in other experimental settings of NAFLD/NASH begins to reveal how exposure to TCDD and other AhR ligands may impact the mechanistic progression of NAFLD in humans.

SUPPLEMENTARY DATA

Supplementary data are available online at http://toxsci.oxfordjournals.org/.

ACKNOWLEDGMENTS

The authors would like to thank Holly Cline-Fedewa for her assistance in the management of the mouse colony.

FUNDING

National Institutes of Health (NIH R01 ES017537 to J.P.L.); National Institute of Environmental Health Sciences Superfund Research Program (NIEHS SRP P42ES04911) and AgBioResearch at MSU (to T.R.Z.); MSU Barnett Rosenberg Endowed Assistantship and Integrative Training in the Pharmacological Sciences grant (NIH 5T32GM092715 to R.N.). Canadian Institutes of Health Research (CIHR) Doctoral Foreign Study Award (DFS-140386 to K.A.F.).

REFERENCES

Cave, M., Appana, S., Patel, M., Falkner, K. C., McClain, C. J., and Brock, G. (2010). Polychlorinated biphenyls, lead, and mercury are associated with liver disease in American adults: NHANES 2003-2004. *Environ. Health Perspect.* **118**, 1735–1742.

Connolly, A. J., Suh, D. Y., Hunt, T. K., and Coughlin, S. R. (1997). Mice lacking the thrombin receptor, PAR1, have normal skin wound healing. *Am. J. Pathol.* **151**, 1199–1204.

Esmon, C. T. (2005). The interactions between inflammation and coagulation. *Br. J. Haematol.* **131**, 417–430.

Fader, K. A., Nault, R., Ammendolia, D. A., Harkema, J. R., Williams, K. J., Crawford, R. B., Kaminski, N. E., Potter, D., Sharratt, B., and Zacharewski, T. R. (2015). 2,3,7,8-Tetrachlorodibenzo-p-dioxin alters lipid metabolism and depletes immune cell populations in the jejunum of C57BL/6 mice. *Toxicol. Sci.* **148**, 567–580.

Fernandez-Salguero, P. M., Hilbert, D. M., Rudikoff, S., Ward, J. M., and Gonzalez, F. J. (1996). Aryl-hydrocarbon receptor-deficient mice are resistant to 2,3,7,8-tetrachlorodibenzo-p-dioxin-induced toxicity. *Toxicol. Appl. Pharmacol.* **140**, 173–179.

Fiorucci, S., Antonelli, E., Distrutti, E., Severino, B., Fiorentina, R., Baldoni, M., Caliendo, G., Santagada, V., Morelli, A., and Cirino, G. (2004). PAR1 antagonism protects against experimental liver fibrosis. Role of proteinase receptors in stellate cell activation. *Hepatology* **39**, 365–375.

Ford, E. S., Li, C., and Zhao, G. (2010). Prevalence and correlates of metabolic syndrome based on a harmonious definition among adults in the US. *J. Diabetes* **2**, 180–193.

Gaca, M. D., Zhou, X., and Benyon, R. C. (2002). Regulation of hepatic stellate cell proliferation and collagen synthesis by proteinase-activated receptors. *J. Hepatol.* **36**, 362–369.

Joshi, N., Kopec, A. K., Ray, J. L., Cline-Fedewa, H., Nawabi, A., Schmitt, T., Nault, R., Zacharewski, T. R., Rockwell, C. E., Flick, M. J., and Luyendyk, J. P. (2016). Fibrin deposition following bile duct injury limits fibrosis through an alphaMbeta2-dependent mechanism. *Blood* **127,** 2751–2762.

Kahn, M. L., Nakanishi-Matsui, M., Shapiro, M. J., Ishihara, H., and Coughlin, S. R. (1999). Protease-activated receptors 1 and 4 mediate activation of human platelets by thrombin. *J. Clin. Invest.* **103**, 879–887.

Kallis, Y. N., Scotton, C. J., Mackinnon, A. C., Goldin, R. D., Wright, N. A., Iredale, J. P., Chambers, R. C., and Forbes, S. J. (2014). Proteinase activated receptor 1 mediated fibrosis in a mouse model of liver injury: a role for bone marrow derived macrophages. *PLoS One* **9**, e86241.

Kassel, K. M., Owens, A. P., 3rd, Rockwell, C. E., Sullivan, B. P., Wang, R., Tawfik, O., Li, G., Guo, G. L., Mackman, N., and Luyendyk, J. P. (2011). Protease-activated receptor 1 and hematopoietic cell tissue factor are required for hepatic steatosis in mice fed a Western diet. *Am. J. Pathol.* **179**, 2278–2289.

Kassel, K. M., Sullivan, B. P., Cui, W., Copple, B. L., and Luyendyk, J. P. (2012). Therapeutic administration of the direct thrombin inhibitor argatroban reduces hepatic inflammation in mice with established fatty liver disease. *Am. J. Pathol.* **181**, 1287–1295.

Kopec, A. K., Boverhof, D. R., Nault, R., Harkema, J. R., Tashiro, C., Potter, D., Sharratt, B., Chittim, B., and Zacharewski, T. R. (2013). Toxicogenomic evaluation of long-term hepatic effects of TCDD in immature, ovariectomized C57BL/6 mice. *Toxicol. Sci.* **135**, 465–475.

Kopec, A. K., Joshi, N., Towery, K. L., Kassel, K. M., Sullivan, B. P., Flick, M. J., and Luyendyk, J. P. (2014). Thrombin inhibition with dabigatran protects against high-fat diet-induced fatty liver disease in mice. *J. Pharmacol. Exp. Ther.* **351**, 288–297.

Kopec, A. K., and Luyendyk, J. P. (2016). Role of fibrin(ogen) in progression of liver disease: guilt by association? *Semin. Thromb. Hemost.* **42**, 397–407.

Lee, D. H., Lee, I. K., Porta, M., Steffes, M., and Jacobs, D. R. Jr. (2007). Relationship between serum concentrations of persistent organic pollutants and the prevalence of metabolic syndrome among non-diabetic adults: results from the National Health and Nutrition Examination Survey 1999-2002. *Diabetologia* **50**, 1841–1851.

Lee, D. H., Lee, I. K., Song, K., Steffes, M., Toscano, W., Baker, B. A., and Jacobs, D. R. Jr. (2006). A strong dose-response relation between serum concentrations of persistent organic pollutants and diabetes: results from the National Health and Examination Survey 1999-2002. *Diabetes Care* **29**, 1638–1644.

Levene, A. P., Kudo, H., Armstrong, M. J., Thursz, M. R., Gedroyc, W. M., Anstee, Q. M., and Goldin, R. D. (2012). Quantifying hepatic steatosis—more than meets the eye. *Histopathology* **60**, 971–981.

Lindsey, S., Jiang, J., Woulfe, D., and Papoutsakis, E. T. (2014). Platelets from mice lacking the aryl hydrocarbon receptor exhibit defective collagen-dependent signaling. *J. Thromb. Haemost.* **12**, 383–394.

Luyendyk, J. P., Mackman, N., and Sullivan, B. P. (2011). Role of fibrinogen and protease-activated receptors in acute xenobiotic-induced cholestatic liver injury. *Toxicol. Sci.* **119**, 233–243.

Luyendyk, J. P., Sullivan, B. P., Guo, G. L., and Wang, R. (2010). Tissue factor-deficiency and protease activated receptor-1-deficiency reduce inflammation elicited by diet-induced steatohepatitis in mice. *Am. J. Pathol.* **176**, 177–186.

Nault, R., Colbry, D., Brandenberger, C., Harkema, J. R., and Zacharewski, T. R. (2015a). Development of a computational high-throughput tool for the quantitative examination of dose-dependent histological features. *Toxicol. Pathol.* **43**, 366–375.

Nault, R., Fader, K. A., Ammendolia, D. A., Dornbos, P., Potter, D., Sharratt, B., Kumagai, K., Harkema, J. R., Lunt, S. Y., Matthews, J., and Zacharewski, T. R. (2016). Dose-dependent metabolic reprogramming and differential gene expression in mouse TCDD-elicited hepatic fibrosis. *Toxicol. Sci.* doi: dx.doi.org/10.1093/toxsci/kfw163.

Nault, R., Fader, K. A., and Zacharewski, T. (2015b). RNA-Seq versus oligonucleotide array assessment of dose-dependent TCDD-elicited hepatic gene expression in mice. *BMC Genomics* **16**, 373.

Owens, A. P., 3rd, Passam, F. H., Antoniak, S., Marshall, S. M., McDaniel, A. L., Rudel, L., Williams, J. C., Hubbard, B. K., Dutton, J. A., Wang, J., *et al.* (2012). Monocyte tissue factor-dependent activation of coagulation in hypercholesterolemic mice and monkeys is inhibited by simvastatin. *J. Clin. Invest.* **122**, 558–568.

Pierre, S., Chevallier, A., Teixeira-Clerc, F., Ambolet-Camoit, A., Bui, L. C., Bats, A. S., Fournet, J. C., Fernandez-Salguero, P., Aggerbeck, M., Lotersztajn, S., *et al.* (2014). Aryl hydrocarbon receptor-dependent induction of liver fibrosis by dioxin. *Toxicol. Sci.* **137**, 114–124.

Pitsavos, C., Panagiotakos, D., Weinem, M., and Stefanadis, C. (2006). Diet, exercise and the metabolic syndrome. *Rev. Diabet. Stud.* **3**, 118–126.

Rullier, A., Gillibert-Duplantier, J., Costet, P., Cubel, G., Haurie, V., Petibois, C., Taras, D., Dugot-Senant, N., Deleris, G., Bioulac-Sage, P., and Rosenbaum, J. (2008). Protease-activated

receptor 1 knockout reduces experimentally induced liver fibrosis. *Am. J. Physiol. Gastrointest. Liver Physiol.* **294**, G226–G235.

Sullivan, B. P., Kassel, K. M., Manley, S., Baker, A. K., and Luyendyk, J. P. (2011). Regulation of transforming growth factor-beta1-dependent integrin beta6 expression by p38 mitogen-activated protein kinase in bile duct epithelial cells. *J. Pharmacol. Exp. Ther.* **337**, 471–478.

Sullivan, B. P., Weinreb, P. H., Violette, S. M., and Luyendyk, J. P. (2010). The coagulation system contributes to alphaVbeta6 integrin expression and liver fibrosis induced by cholestasis. *Am. J. Pathol.* **177**, 2837–2849.

Taylor, K. W., Novak, R. F., Anderson, H. A., Birnbaum, L. S., Blystone, C., Devito, M., Jacobs, D., Kohrle, J., Lee, D. H., Rylander, L., *et al.* (2013). Evaluation of the association between persistent organic pollutants (POPs) and diabetes in epidemiological studies: a national toxicology program workshop review. *Environ. Health Perspect.* **121**, 774–783.

Unger, R. H., Clark, G. O., Scherer, P. E., and Orci, L. (2010). Lipid homeostasis, lipotoxicity and the metabolic syndrome. *Biochim. Biophys. Acta* **1801**, 209–214.

Unger, R. H., and Scherer, P. E. (2010). Gluttony, sloth and the metabolic syndrome: a roadmap to lipotoxicity. *Trends Endocrinol. Metab.* **21**, 345–352.

Vanni, E., Bugianesi, E., Kotronen, A., De Minicis, S., Yki-Jarvinen, H., and Svegliati-Baroni, G. (2010). From the metabolic syndrome to NAFLD or vice versa? *Dig. Liver Dis.* **42**, 320–330.

Vos, J. G., Moore, J. A., and Zinkl, J. G. (1974). Toxicity of 2,3,7,8-tetrachlorodibenzo-p-dioxin (TCDD) in C57B1/6 mice. *Toxicol. Appl. Pharmacol.* **29**, 229–241.

Weng, H., Mertens, P. R., Gressner, A. M., and Dooley, S. (2007). IFN-gamma abrogates profibrogenic TGF-beta signaling in liver by targeting expression of inhibitory and receptor Smads. *J. Hepatol.* **46**, 295–303.